Journal of Ginseng Research 47 (2023) 645–653

Contents lists available at ScienceDirect

Journal of Ginseng Research

journal homepage: https://www.sciencedirect.com/journal/journal-of-ginseng-research

Research Article

Ginsenoside Rk1 inhibits HeLa cell proliferation through an endoplasmic reticulum signaling pathway

Qiuyang Li [1], Hang Sun [1], Shiwei Liu, Jinxin Tang, Shengnan Liu, Pei Yin, Qianwen Mi, Jingsheng Liu, Lei yu, Yunfeng Bi*

College of Food Science and Engineering, Jilin Agricultural University, Changchun, China

ARTICLE INFO

Article history:
Received 12 May 2022
Received in revised form
5 April 2023
Accepted 8 April 2023
Available online 14 April 2023

Keywords:
Ginsenoside Rk1
Cervical cancer
Protein processing in endoplasmic reticulum
RNA seq

ABSTRACT

Background: Changes to work-life balance has increased the incidence of cervical cancer among younger people. A minor ginseng saponin known as ginsenoside Rk1 can inhibit the growth and survival of human cancer cells; however, whether ginsenoside Rk1 inhibits HeLa cell proliferation is unknown.
Methods and results: Ginsenoside Rk1 blocked HeLa cells in the G0/G1 phase in a dose-dependent manner and inhibited cell division and proliferation. Ginsenoside Rk1 markedly also activated the apoptotic signaling pathway via caspase 3, PARP, and caspase 6. In addition, ginsenoside Rk1 increased LC3B protein expression, indicating the promotion of the autophagy signaling pathway. Protein processing in the endoplasmic reticulum signaling pathway was downregulated in Gene Ontology (GO) and Kyoto Encyclopedia of Genes and Genomes (KEGG) pathway enrichment analyses, consistent with real-time quantitative PCR and western blotting that showed YOD1, HSPA4L, DNAJC3, and HSP90AA1 expression levels were dramatically decreased in HeLa cells treated with ginsenoside Rk1, with YOD1 was the most significantly inhibited by ginsenoside Rk1 treatment.
Conclusion: These findings indicate that the toxicity of ginsenoside Rk1 in HeLa cells can be explained by the inhibition of protein synthesis in the endoplasmic reticulum and enhanced apoptosis, with YOD1 acting as a potential target for cervical cancer treatment.

1. Introduction

Cervical cancer is a common gynecological malignant tumor that occurs in people aged 35–55 years, but has been increasing among young women because of changes in living habits and professional stress [1]. Epidemiological studies have shown that HeLa cells are closely associated to human papillomavirus infection and defects in immune function [2]. Early symptoms of cervical cancer are atypical, with most patients already presenting an advanced stage of disease when they are diagnosed and miss the best opportunity for surgery, requiring chemotherapy to kill tumor cells [3].

Ginseng has many pharmacological effects, such as anti-aging [4], antitumor, antineuralgic [5], antidepressant, and immune regulation [6]. Ginsenosides are the main active ingredients of ginseng and have been intensively evaluated in pharmacological studies. Previous studies have shown that Rk1 significantly reduces telomerase activity, limits cellular development, and causes morphological abnormalities. The synchronization of telomerase activity inhibition with apoptosis induction is the basis for the antitumor effect of Rk1 [7]; however, it remains unknown whether ginsenoside Rk1 inhibits cervical cancer cell proliferation.

Traditional research primarily adopts biochemical and molecular methods to collect relevant information on cancer proliferation etc. However, this strategy has a low throughput and requires cumbersome operations. RNA sequencing (RNA-seq) uses cDNA libraries reverse-transcribed from RNA isolated from tissues using high-throughput sequencing technology [8] to quickly and accurately screen relevant gene expression information. Rk1 is a potent inhibitor of cell growth and induced cancer cell apoptosis in this study's *in vitro* cell studies. RNA-seq transcriptome sequencing revealed that different signaling pathways and genes were expressed after treatment with ginsenoside Rk1. The biological processes regulated by ginsenoside Rk1 were investigated by

* Corresponding author. Jilin Agricultural University, 130118, China. Tel.: 13039019618.
E-mail addresses: liujs1007@vip.sina.com.cn (J. Liu), yulei@jlau.edu.cn (L. yu), yunfeng5609@sohu.com (Y. Bi).
[1] The first two authors contributed equally to this work.

https://doi.org/10.1016/j.jgr.2023.04.004

western blotting and real-time quantitative PCR (RT-qPCR). This study indicates that ginsenoside Rk1 can be used to inhibit regeneration and promote apoptosis in HeLa cells.

2. Materials and methods

2.1. Materials and instruments

The phosphate-buffered saline (PBS), CCK 8 kit, cell cycle detection kit, CHC13, enzyme-free sterile water, and apoptosis detection kit were purchased from Beijing Suo Laibao Technology Co., Ltd. Ginsenoside Rk1 was purchased from Jinsheng Biotechnology Co. Ltd. Caspase 3, PARP, caspase 6, LC3B, YOD1, HSPA4L, DNAJC3, and HSP90AA1 were purchased from Beijing Boasen Biological Co. Ltd. Fetal bovine serum (FBS) was supplied by Beijing Baiao Laibo Technology Co., Ltd.; PVDF membranes were procured from Millipore. The reverse transcriptase (1896649) and R0133DUTP solutions were provided by Invitrogen. SuperScript™ II Reverse Transcriptase, m0209, and *Escherichia coli* DNA polymerase I were acquired from Ambion. The AHTS chain mRNA SEQ library preparation kit and phenol-chloroform were purchased from Thermo Fisher Technology Co., Ltd. (China). A nucleic acid purification kit was purchased from Aide Technology Co., Ltd., the one-step SYBR Green PCR reagent kit was obtained from Yeasen, and all other reagents were of analytical grade. The instruments used were provided by the processing and utilization teams of the new food resources.

2.2. Cell resuscitation and culture

The HeLa cell line was purchased from Delta Biotechnology Co., Ltd. The cell masses were gently cultured to form single-cell suspensions. The single cell suspension was homogenized in a shaking dish and cultured in an incubator with 5% CO_2 at 37°C as previously described [9].

2.3. Inhibitory effects of ginsenoside Rk1 on HeLa cells

HeLa cells were plated in a 96-well plate at a density of 1×10^5 cells per well and incubated for 24 h at 37°C with 5% CO_2. The cells were then grown for 24 h with 1, 2, 4, 8, 10, 20, and 30 μM ginsenoside Rk1. Following the addition of 10 μL CCK 8 solution, the cells were incubated at 37°C for 1 h in the dark. A microplate reader was used to measure absorbance at 450 nm. The changes in cell viability before and after Rk1 administration were calculated using the following formula:

$$\text{Cell viability } (\%) = (\text{OD [Rk1 group]} - \text{OD [blank group]} \times) / (\text{OD [control]} - \text{OD [blank group]}) \times 100\%$$

2.4. Apoptosis detection

Apoptosis was detected using the Hoechst staining kit. The cells were fixed in a 4% paraformaldehyde solution for 2 h after administration, and the fixing solution was removed. Cells were rinsed with phosphate-buffered saline (PBS) solution for 3 min and then removed. The cells were incubated with Hoechst 33258 stain for 5 min and blue nuclei were detected under a fluorescence microscope.

The HeLa cells were administered 10, 20, or 30 μM ginsenoside Rk1, digested with 0.25% trypsin without EDTA, and then rinsed with precooled PBS solution. Annexin V was labeled with fluorescein isothiocyanate (annexin V-FITC) and used as the fluorescent probe to detect apoptosis by flow cytometry.

2.5. Differential gene expression

Differentially expressed mRNAs were chosen with a fold change of > 2 or a fold change of < 0.5 and a p value of < 0.05 using the R package edge R.

2.6. Gene Ontology and pathway enrichment analyses

The Kobas 2.0 server determined the functional categorization, GO terms, and KEGG pathways of the identified differentially expressed genes (DEGs). Molecular functions, cellular components, and biological processes were the three ontologies comprising the GO term analysis.

To discover the pathways that were considerably enriched in the significantly differentially expressed genes when compared to the background of the entire genome, significant enrichment analysis of the pathway used the KEGG pathway as the unit and performed a hypergeometric test.

2.7. RT qPCR

Total RNA was extracted and purified using TRIzol reagent following the manufacturer's instructions. The quantity and quality of the RNA in each sample were determined using a NanoDrop ND 1000 spectrophotometer. A Bioanalyzer 2100 (RIN score > 7.0) was used to analyze the integrity of RNA, and denaturing agarose gel electrophoresis was used to confirm the results. Using Dynabeads Oligo (dT)25 61005 and two rounds of purification, poly(A) RNA was isolated from 1 g total RNA. Then, the Magnesium RNA Fragmentation Module was used to digest the poly(A) RNA at 94°C for 5-7 min. The reverse-transcribed cDNA was then diluted ten-fold with RNase-free dH_20 after the RNA was fragmented. The PCR reaction system included l0 μL each forward and reverse primers, 80 μL RNase free dH_20, 10 μL SYBR qPCR mix, 1 μL sample cDNA, 1.6 μL primer mixture, and 7.4 μL enzyme free water. Using the $2^{-\Delta\Delta CT}$ approach, the relative gene expression level was calculated. Each sample was run in triplicate.

2.8. Western blotting analysis

In brief, the cells were collected with trypsin and fully digested with pyrolysis fluid at 4°C. The lysate was centrifuged for 15 min at 12,000 rpm at 4°C. The supernatant was collected and protein concentration was determined using a BCA kit. The supernatant was then mixed with 10 μL 12% SDS and heated for 5 min before SDS PAGE electrophoresis. After washing with PBST for 5 min, the membranes was incubated with 5% skim milk (in TBST) for 1.5 h. The membranes were washed with PBST for 5 min and then incubated in caspase 3, caspase 6, PARP, LC3B, or GAPDH antibody (diluted to 1:1,000) in a chromatography cabinet at 4°C for 12 h. The PVDF membranes were then treated with a secondary antibody (1:10,000) that had been tagged with horseradish peroxidase at 37°C for 1.5 h. Chromogenic analysis was performed using an ECL chemiluminescence-photoluminescence kit and a multipurpose gel imaging system.

2.9. Statistical analyses

Each experiment was conducted at least three times and all data are shown as the mean ± SD. Statistical analyses were carried out using Origin 8.5 and Microsoft Excel. A Tukey's test and one-way

ANOVA were used to assess the differences between the groups at $p < 0.05$, which was considered statistically significant [10].

3. Results and analyses

3.1. Inhibitory effects of ginsenoside Rk1 on HeLa cell growth

HeLa cells treated with ginsenoside Rk1 for 8, 16, and 24 h indicated that ginsenoside Rk1 inhibited HeLa cell growth in dose- and time-dependent manners (Fig. 1 A). After 24 h, the inhibition of HeLa cell growth increased from 15.1% to 30.3% as ginsenoside Rk1 concentration increased from l0 -30 μM.

3.2. Effects of ginsenoside Rk1 on HeLa cell morphology

In the control group, HeLa cells had almost no apoptotic cells and were uniform and complete, with clear edges (Fig. 1 B). After treatment with different concentrations of ginsenoside Rk1, the morphology of the cells changed; the cells shrank and became marginalized and their size decreased considerably, indicating apoptosis. The numbers of cells markedly decreased when the concentration of ginsenoside Rk1 was over 30 μM. These data suggested that Rk1 and Rh1 induced apoptosis.

3.3. Effects of ginsenoside Rk1 on HeLa cell cycle

Ginsenoside Rk1 dose-dependently inhibited HeLa cells in the G0/G1 phase of the cell cycle (Fig. 1 C and 1 D). Moreover, 20 μM and 30 μM ginsenoside Rk1 significantly increased the cell content in the G0/G1 phase ($p < 0.01$) and then reduced the cell content in the S and the G2/M phases. These results showed that ginsenoside Rk1 exerted an inhibitory effect on cell division, delaying tumor cell growth and reducing cell proliferation.

3.4. Effects of ginsenoside Rk1 on HeLa cell apoptosis

To determine the effect of ginsenoside Rk1 on HeLa cell apoptosis, changes in the cell shape were observed in cell cultures treated with and without Rk1 (Fig. 2 A). The morphology of HeLa cells treated with ginsenoside Rk1 showed typical apoptotic characteristics, including smaller chromatin, bright blue nuclei, and a high proportion of bright blue fragments.

To further investigate the effects of ginsenoside Rk1 on HeLa cell apoptosis, annexin V/PI double labeling was measured using flow cytometry, which showed that ginsenoside Rk1 treatment groups underwent more apoptosis than those in the control group (Fig. 2 B and 2 C). A correlation was observed between the percentage of apoptosis rate, which increased from 4.28 ± 0.47% to 12.39 ± 0.99% ($p < 0.001$), and ginsenoside Rk1 content. These results indicated that ginsenoside Rk1 mainly inhibited HeLa cell proliferation via the apoptotic pathway.

3.5. Ginsenoside RK1 affects immune protein expression

Western blotting was used to evaluate the expression of several apoptosis-related proteins, including caspase 3, caspase 6, PARP, and LC3B, in response to ginsenoside Rk1 treatment in HeLa cells. The ginsenoside Rk1 treatment groups had higher expression levels of caspase 3, caspase 6, PARP, and LC3B than the control group (Fig. 3 A and B). In the ginsenoside Rk1 treatment groups, the expression of caspase 3 and caspase 6 significantly increased($p < 0.05$). We also found that HeLa cells treated with 20 and 30 μM ginsenoside Rk1 gradually enhanced the expression levels of

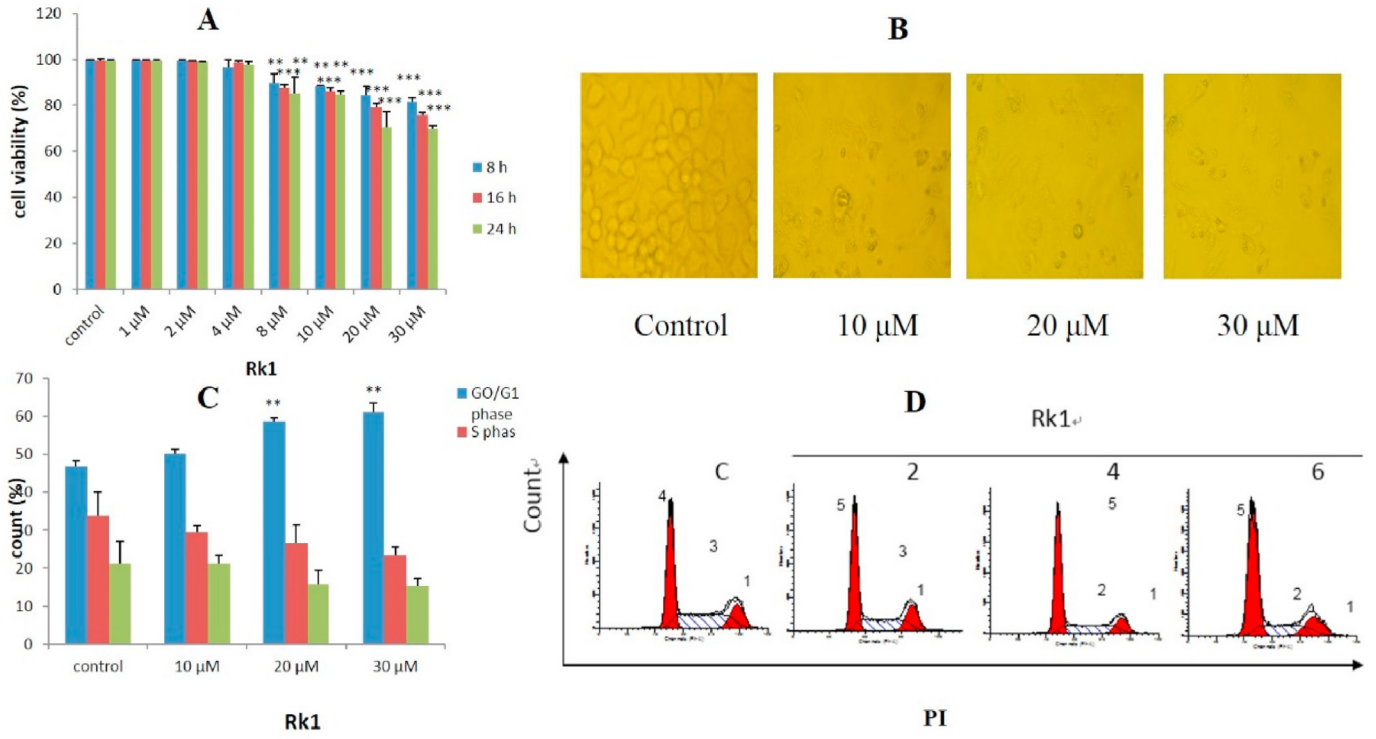

Fig. 1. Effect of ginsenoside RK1 on HeLa cells (A) As the dose and duration of ginsenoside Rk1 treatments increase, the growth rate of Hela cells is inhibited. (B) Effects of ginsenoside Rk1 on HeLa cell morphology. Ginsenoside Rk1 can inhibit the growth of cancer cells. (C) and (D) Effects of ginsenoside Rk1 on HeLa cell cycle. Ginsenoside Rk1 reduced cell proliferation by inhibiting cell division and decreased their proliferative activity in HeLa cells. Compared with the blank control group, *p < 0.05, **p < 0.01, ***p < 0.001.

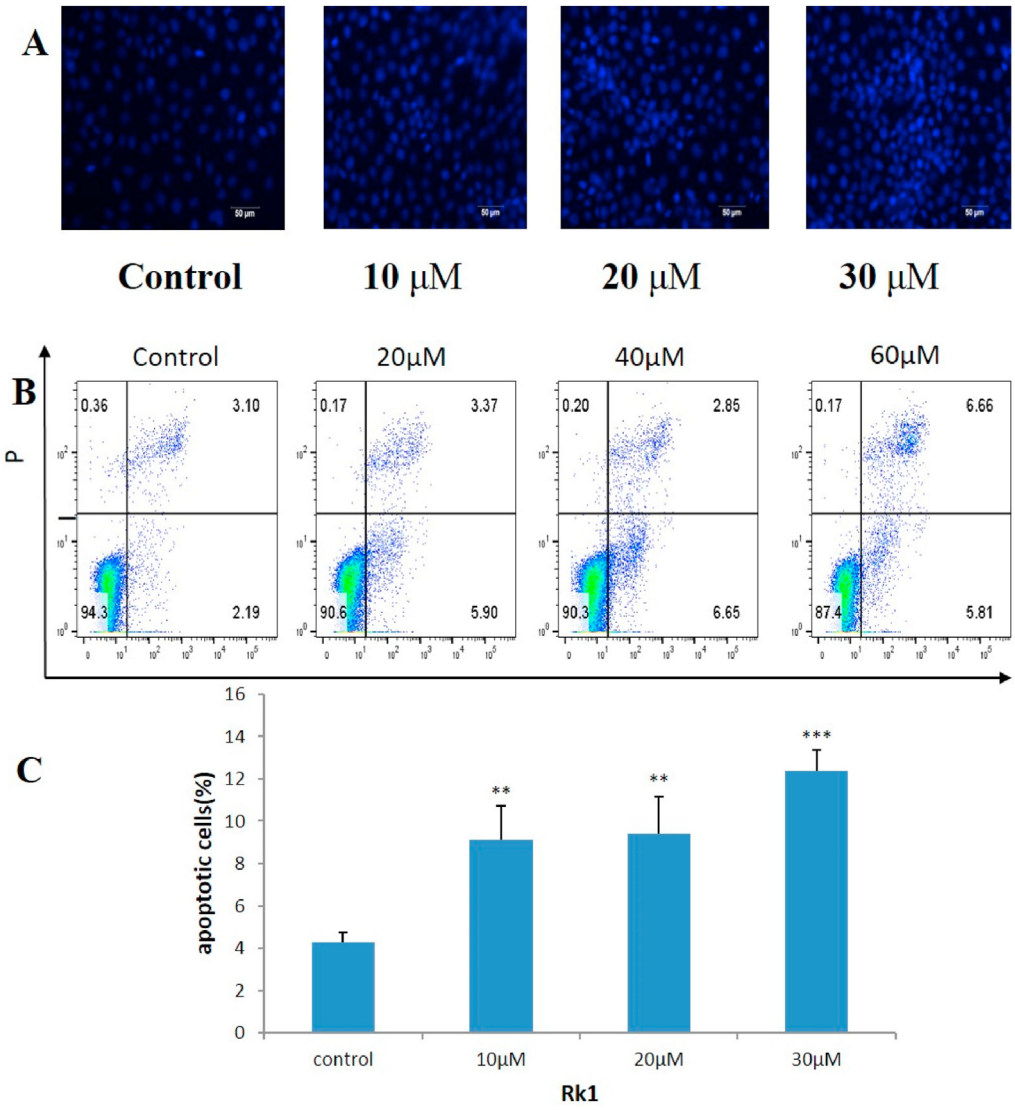

Fig. 2. Effects of ginsenoside Rk1 on HeLa cell apoptosis (A) The effects of ginsenoside Rk1 on HeLa cell apoptosis via cell morphology. After ginsenoside Rk1 administration, the proportion of bright blue nuclei increased significantly, indicating induced apoptosis. (B) Scatter plot from the flow cytometry analysis. (C) With the increase of Rk1 concentration, the apoptosis rate of treated HeLa cells significantly increased compared with the untreated control. Compared with the blank control group, *p < 0.05, **p < 0.01, ***p < 0.001.

PARP and LC3B in a dose-dependent manner ($p < 0.01$), suggesting ginsenoside Rk1 promoted apoptosis through the activation of the apoptotic signaling pathways that involve caspase 3, PARP, and caspase 6. Moreover, these results showed that ginsenoside Rk1 promoted autophagy of the HeLa cells through LC3B-dependent signaling pathways.

3.6. Rk1 treatment alters gene expression in HeLa cells

Four groups of control and ginsenoside Rk1-treated cells were established to evaluate the effects of ginsenoside RK1 treatment on human HeLa cells. Total RNA from the four sample groups was prepared as cDNA libraries and sequenced to obtain high-quality transcriptome data. Analysis of the quality of the clean data revealed that the average value of the base quality (Q30) was 98.3% and the average proportion of effective reads was 97.52%. Therefore, the sequencing results were considered to be accurate and reliable.

3.7. Volcano map analysis of DEGs

The overall distribution of the differentially expressed genes (DEGs) can be understood as a volcano map. The responsiveness of these genes to Rk1 therapy was evaluated by comparing the differential expression of the genes in the treatment and control samples. Using FC $\geq$ 2 and FDR < 0.05 as the criteria, 4,113 DEGs were identified between the control and 10 μM ginsenoside Rk1 treated groups (Fig. 4 A). These DEGs included 187 upregulated and 3,926 downregulated genes. Additionally, 5,016 DEGs between the control and 20 μM ginsenoside Rk1 treated groups were found, which included 534 upregulated and 4,482 downregulated genes. Additionally, between the control and 30 μM ginsenoside Rk1

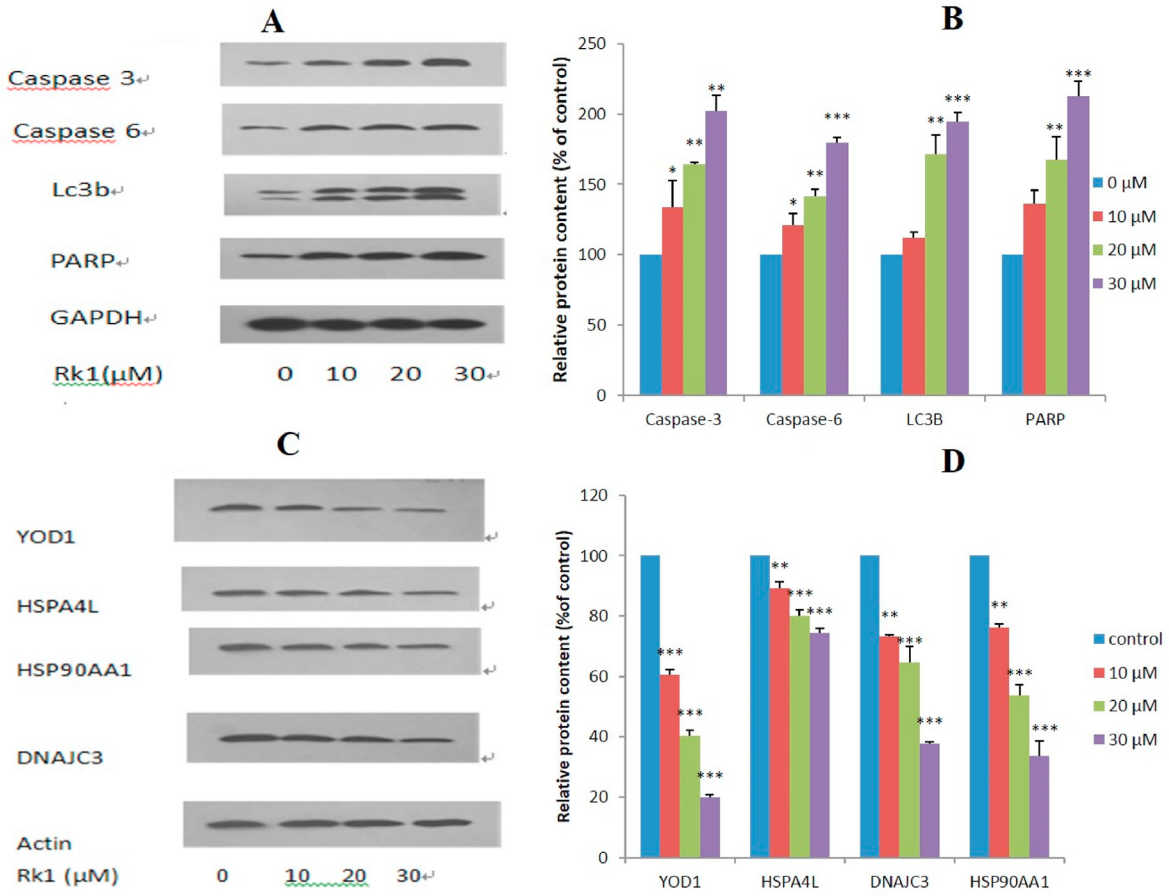

Fig. 3. Protein expression levels in HeLa cells after ginsenoside Rk1 treatment (A) and (B) Protein expression of caspase 3, caspase 6, PARP, and LC3B in HeLa cells is significantly increased after ginsenoside Rk1 treatment when compared with the untreated control. (C) and (D) Protein expression of YOD1, HSPA4L, DNAJC3, and HSP90AA1 in HeLa cells after ginsenoside Rk1 treatment is significantly reduced when compared with the untreated control. Among all proteins, YOD1 was the most significantly inhibited by Rk1; its expression was downregulated by nearly 5-fold compared to that of the control. Compared to the blank control group, *$p < 0.05$, **$p < 0.01$, ***$p < 0.001$.

treated groups, 5,438 DEGs were found, of which 766 were upregulated and 4,582 were downregulated.

3.8. GO enrichment analysis of DEGs associated with ginsenoside Rk1 treatment

Three GO term categories were annotated for each DEG group: molecular functions, cellular components, and biological processes. The top 50 functionally-enriched classes in each group were primarily enriched for protein binding, metal ion binding, and DNA binding in terms of molecular activities (Fig. 5). DEGs were largely abundant in the membrane, cytoplasm, and nucleus of the biological components, as well as the cell cycle, DNA template, positive regulation of transcription by RNA polymerase II, and regulation of transcription. Consistent with previous studies, the present data also showed that HeLa cells were significantly enriched in signaling pathways, such as material transport, cytoskeleton components, protein folding, cell cycle, and apoptosis when compared to normal cervical tissues.

3.9. KEGG pathway enrichment analysis of DEGs in response to ginsenoside Rk1 treatment

In organisms, various genes work together to perform biological functions. It would be beneficial to further understand the biological functions of these genes via pathway-based analyses. The primary online database for pathways is called KEGG.

Most genes related to the cell cycle (e.g., *CDC27*, *GSK3B*, *TGFB2*, *CDC6*, *CDC23*, and *CDC7*) were highly enriched in cell proliferation-related pathways (Fig. 6). Moreover, genes involved in signaling pathways related to cell aging, such as *CCNA2*, *CDKN2B*, *ATM*, *CHEK1*, *FOXO1*, and *ITPR1*, were also significantly enriched in cell cycle genes DEGs associated with Rk1 treatment. Furthermore, one of the most significantly enhanced signaling pathways among the three ginsenoside Rk1 concentrations was protein processing in the endoplasmic reticulum signaling pathway. In this pathway, some "star" genes, such as *YOD1*, *HSPA4L*, *DNAJC3*, and *HSP90AA1*, were downregulated. These genes are related to endoplasmic reticulum protein processing and transportation and are also closely related to apoptosis resistance.

3.10. Hierarchical clustering of DEGs in the endoplasmic reticulum signaling pathway

All DEGs involved in protein processing in the endoplasmic reticulum signaling pathway were tested for ten pathway-related genes and listed in a hierarchical cluster diagram (Fig. 4 B). All of these DEGs (e.g., *SSR3*, *SSR1*, *HSPA4L*, *HSP90AA1*, *STTSB*, *YOD1*, *DNAJC3*, *UBQLN1*, *DNAJA1*, and *DNAJC10*) were downregulated.

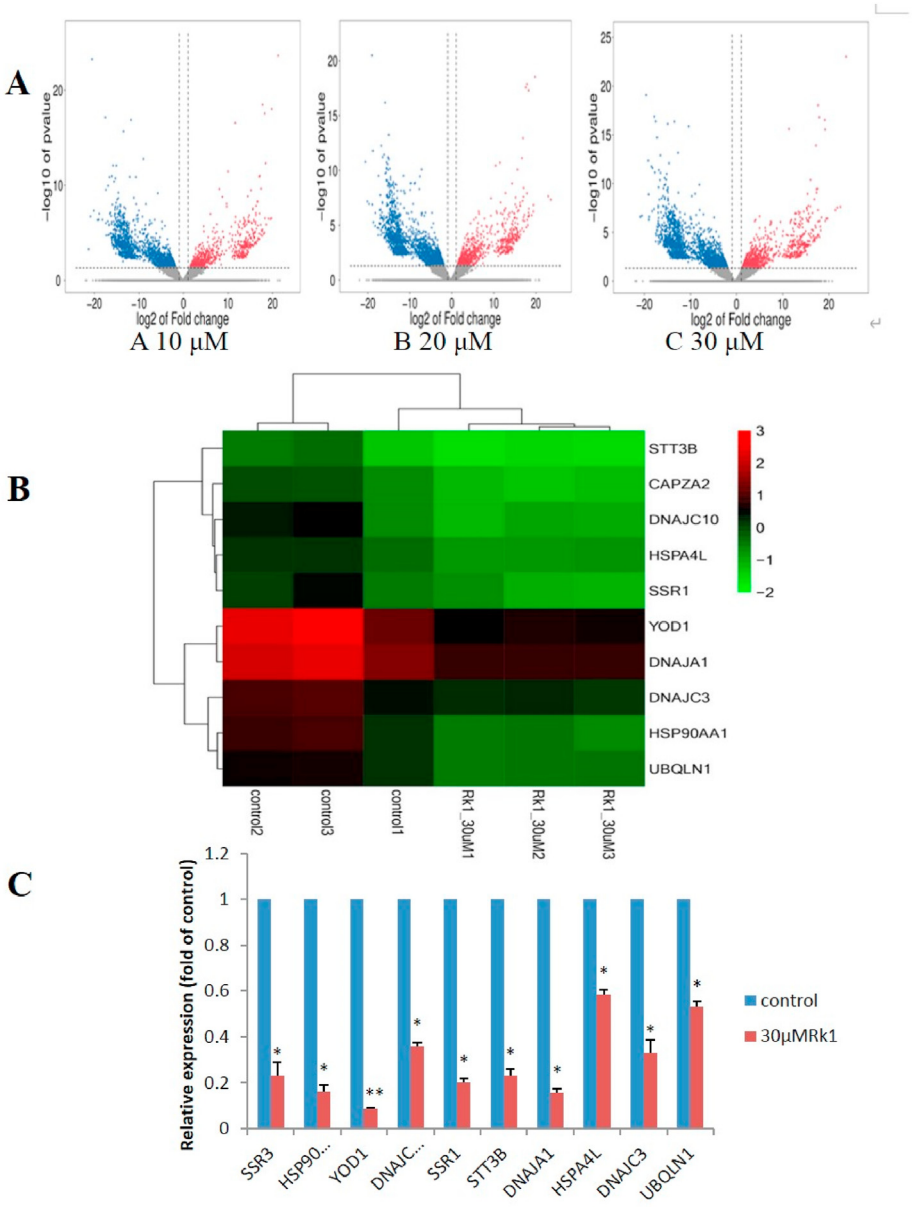

Fig. 4. Differential gene expression after ginsenoside Rk1 treatment (A) An MA plot of levels of differential gene expression in HeLa cells treated with ginsenoside RK1. The response of genes to ginsenoside Rk1 treatment was assessed by determining their differential gene expression between treated and untreated samples. The total number of differentially expressed genes (DEGs) in response to ginsenoside Rk1 treatment in Hela cells increased significantly with ginsenoside Rk1 concentration. (B) A heat map of representative DEGs. The darker the color, the more significant the change in gene expression. (C) Ten DEGs related to protein processing in the endoplasmic reticulum signaling pathway (SSR3, SSR1, YOD1, HSPA4L, HSP90AA1, STTSB, DNAJC3, UBQLN1, *DNAJA1*, and *DNAJC10*) were selected for RT-qPCR. Compared with other genes studied, *YOD1* expression was inhibited by ginsenoside Rk1 treatment, but also showed stable expression in western blotting and RT-qPCR validation experiments, consistent with the RNA-seq results.

3.11. RT-qPCR analysis of associated with ginsenoside Rk1 treatment

We performed RT-qPCR to confirm the accuracy of the RNA-seq results. Ten DEGs involved in protein processing in the endoplasmic reticulum signaling pathway (e.g., *SSR3, SSR1, YOD1, HSPA4L, HSP90AA1, STTSB, DNAJC3, UBQLN1, DNAJA1*, and *DNAJC10*) were selected for RT-qPCR analyses and confirmed to be significantly downregulated ($p < 0.05$) (Fig. 4 C). Notably, the expression of *YOD1* was significantly inhibited ($p < 0.01$) in response to ginsenoside Rk1 treatment, consistent with the trend of change after *YOD1* standardization in the hierarchical cluster diagram of DEGs (Fig. 4 B). These findings supported the hypothesis that ginsenoside Rk1 controls the expression of genes involved in protein synthesis in the endoplasmic reticulum signaling pathway.

3.12. Western blotting analysis of associated with ginsenoside Rk1 treatment

Western blotting was performed to determine the protein levels of genes related to the endoplasmic reticulum signaling pathway. These findings were used to extrapolate the effects of ginsenoside Rk1 on protein processing in the endoplasmic reticulum and apoptosis suppression in HeLa cells. The expression levels of *YOD1*, *HSPA4L*, *DNAJC3*, and *HSP90AA1* were significantly lower in the ginsenoside Rk1 treatment groups were significantly lower than in

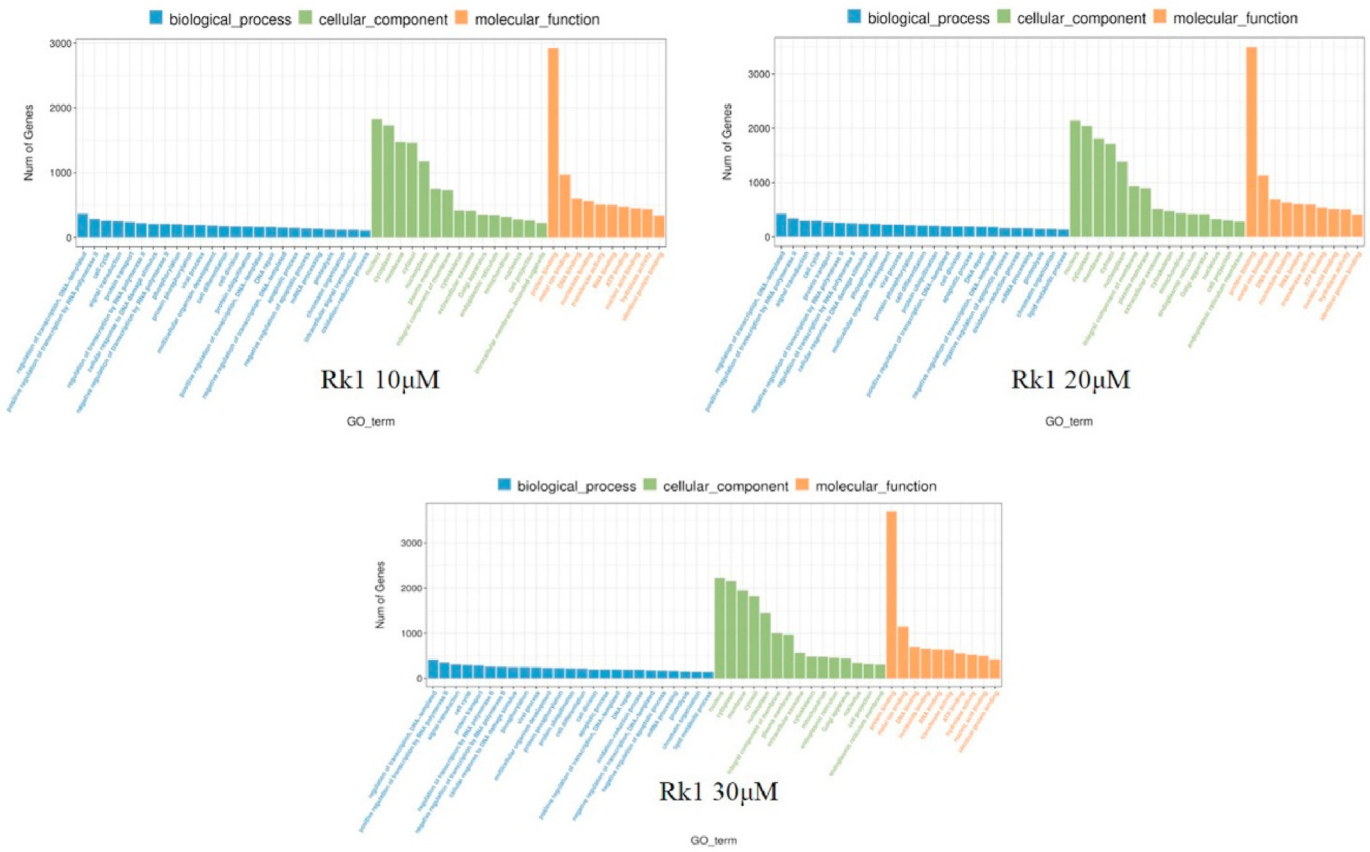

Fig. 5. GO enrichment map of DEGs associated with ginsenoside Rk1 treatment. Each group of DEGs was annotated into three classifications: molecular functions, cellular components, and biological processes. In descending order from large to small, select the GO Term of top 25, top 15 and top 10 respectively for drawing display.

the untreated groups (Fig. 3 C and D). As the ginsenoside Rk1 concentration increased, the expression levels of these proteins gradually decreased, indicating a dose-dependent toxicity effect of ginsenoside Rk1 on HeLa cells. The higher the concentration of ginsenoside Rk1, the more obvious its inhibitory effects on protein synthesis and processing and on genes related to anti-apoptosis. The expression of *YOD1* was most significantly inhibited by ginsenoside Rk1 ($p < 0.001$). Additionally, compared to *HSPA4L*, *DNAJC3*, and *HSP90AA1*, whose expression was downregulated approximately three-fold, *YOD1* expression was nearly five-fold lower ($p < 0.01$). These findings suggested that the endoplasmic reticulum protein production inhibition and anti-apoptotic effects of ginsenoside Rk1 could account for it toxicity in HeLa cells.

4. Discussion

Cervical cance is the fourth most frequent cancer in women globally [11], and in China it is also the most frequent malignant tumor of the female reproductive system. The cure rate for early cervical cance is high, but once metastasis or recurrence occurs, recovery is poor [12]. It was reported that 20 (S) ginsenoside Rh2 triggered protective autophagy and increased the death of cervical cancer cells by blocking the AMPK/mTOR pathway [13], and that ginsenoside Rg5 could inhibit the activation of NFκB by suppressing its upstream kinase transforming growth factor β-activated kinase 1 in TNF-α-treated HeLa or A549 cells [14]. Ginsenoside Rk1 is the major component of ginseng and we found it suppressed cell growth in a dose- and time-dependent manner in HeLa cell cultures. Hoechst 33258 fluorescence staining demonstrated that the number of apoptotic cells increased with increasing ginsenoside Rk1 concentration. Among all caspase families, caspase 3 is an important apoptosis effector that can lead to cytoskeletal rupture, nuclear death, and other apoptosis-related cell changes [15]. PARP is also an important index of activated caspase 3 during apoptosis [16], while caspase 6 functions downstream protein in this cascade reaction [17]. When stimulated by an apoptotic signal, it activates upstream proteins and modifies their active forms to induce cell apoptosis. LC3 is the core component of autophagy and its function is to transport autophagy signals/factors [18]. Western blotting analysis between control and ginsenoside Rk1 treated cells showed that the protein expression of PARP, caspase 6, caspase 3, and LC3B substantially increased in the treated cells when compared to the untreated control, indicating that ginsenoside Rk1 activated the apoptotic signaling pathways of caspase 3, PARP, and caspase 6 to promote apoptosis. Moreover, ginsenoside Rk1 considerably increased the expression of the autophagy marker LC3B, indicating that ginsenoside Rk1 promoted autophagy in HeLa cells through the autophagy signaling pathway.

Inhibition of the occurrence of cervical tumor cells involves multiple factors, several steps, and complex biological processes, in which multiple gene mutations and abnormal expression occur [19]. In this study, DEGs from HeLa cells were assessed using RNA-seq and functional enrichment analysis. The endoplasmic reticulum is not only the organelle responsible for protein folding in cells [20,21], but it also participates in the storage site of intracellular calcium ions [22] and the molecular chaperones for storing and regulating protein folding [23]. These molecules are crucial in determining the sensitivity of cells to apoptosis and endoplasmic

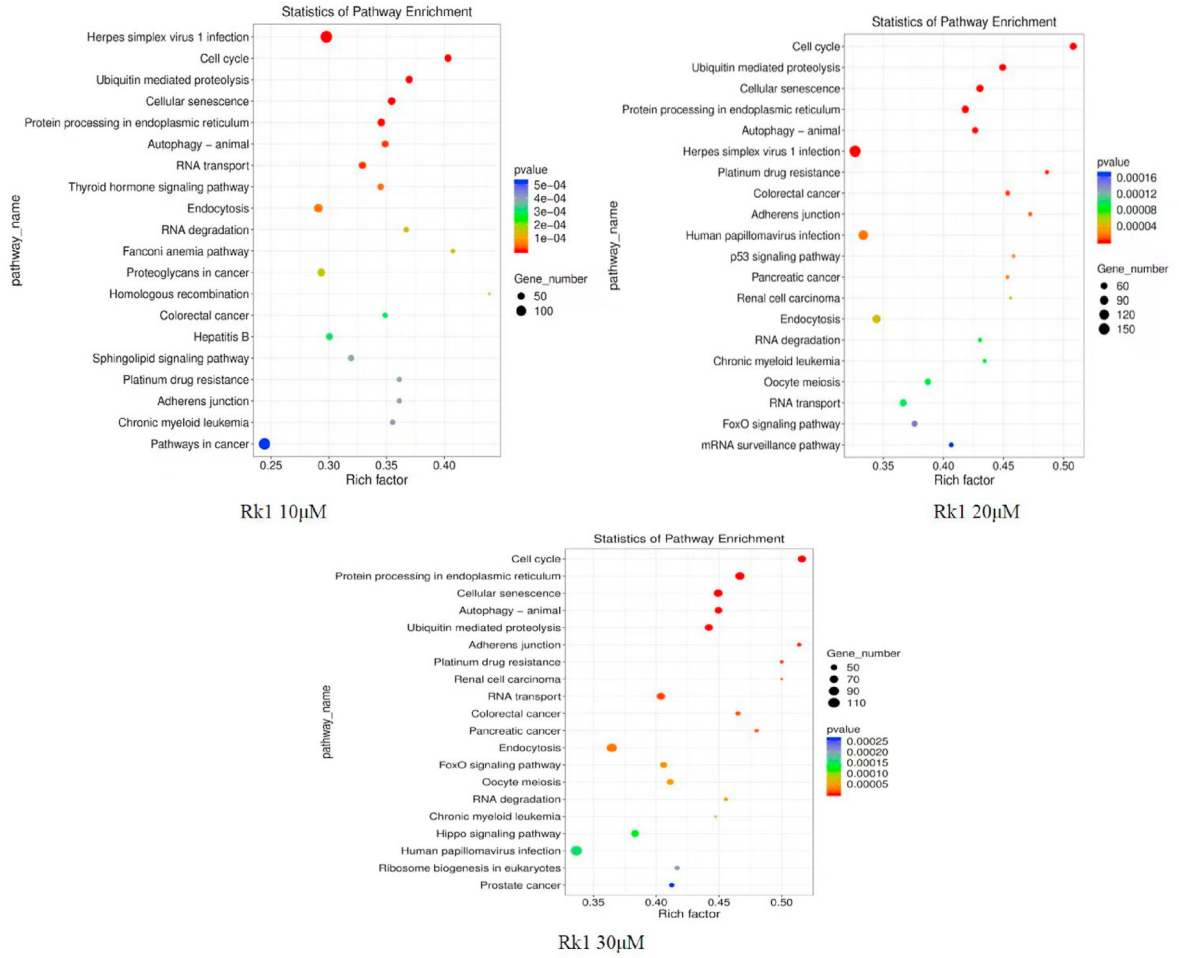

Fig. 6. KEGG pathway analysis of DEGs enriched in response to ginsenoside Rk1 treatment. The horizontal axis represents the enrichment factor and the vertical axis represents the enriched KEGG pathway. The dot size indicates the number of DEGs enriched in a KEGG pathway. Dot colors represent different p-values associated with the DEGs. The enrichment factor indicates the number of DEGs in a KEGG pathway/the total number of genes belonging to this KEGG pathway. The larger the enrichment factor, the higher the enrichment degree for that KEGG pathway.

reticulum stress. The quality control system of the endoplasmic reticulum includes several molecular chaperones that help fold proteins correctly and transport them through the endoplasmic reticulum. Moreover, these chaperones can detect and refold misfolded proteins. If refolding cannot be completed, misfolded proteins are transported for degradation via the proteasome or autophagy pathways [24]. When the number of misfolded proteins exceeds a biological limit, they exert toxic effects and activate apoptosis signals that lead to cell death. Notably, some “hot” genes were downregulated in HeLa cells after drug interference in this pathway. These genes include *YOD1*, *HSPA4L*, *DNAJC3*, and *HSP90AA1*. *YOD1* is a protein ubiquitination gene that was previously reported to be highly expressed in hysteromyoma cells [25], *HSPA4L* is a newly discovered oncogene in pheochromocytoma [26], *DNAJC3* is highly expressed in breast cancer cells [27], and *HSP90AA1* is a relatively “hot” multiple tumor target gene that is not only related to the processing and transportation of endoplasmic reticulum proteins but also closely related to apoptosis resistance [28]. Although the endoplasmic reticulum protein folding effects of ginsenoside Rk1 in HeLa cells can be regulated by pertinent targets, it remains unclear whether these genes are related to the occurrence and development of cervical cancer in clinical conditions.

Notably, the expression levels of the associated proteins decreased as the ginsenoside Rk1 concentration increased, indicating that ginsenoside Rk1 affects HeLa cells in a dose-dependent manner. The higher the concentration of ginsenoside Rk1, the more obvious its inhibitory effects on the control of protein synthesis and processing and the expression of genes related to anti-apoptosis pathways. In addition, *YOD1* expression was significantly inhibited by ginsenoside Rk1 ($p < 0.001$); its expression was downregulated nearly five-fold that of the untreated control. *YOD1* expression was reduced from approximately 0.5 before treatment to approximately 0.1 after treatment at the highest concentration of ginsenoside Rk1. These results showed that the cytotoxicity of ginsenoside Rk1 in HeLa cells was explained by the inhibition of protein synthesis in the endoplasmic reticulum and anti-apoptosis gene expression, consistent with previous studies.

The findings from the RNA-seq analysis discovered that *YOD1* was not only significantly reduced in response to ginsenoside Rk1 treatment, but that it also had a steady expression. Therefore, YOD1 is a potential target for the clinical treatment of cervical cancer.

Author contributions

Qiuyang Li: writing review and editing, data collation; Hang Sun: writing review and editing, data collation; Jinxin Tang: formal analysis; Shiwei Liu: software; Shengnan Liu: review and editing;

Jingsheng Liu: Validation; Bi Yunfeng: conceptualization, review and editing; Yu Lei: project management.

Declaration of competing interest

The authors declare that they have no known competing financial interests or personal relationships that could have appeared to influence the work reported in this paper.

Acknowledgments

This work was partly supported by Science and Technology Department of Jilin Province, China, for providing financial support (20210204179YY).

References

[1] Satari M, Javani JF, Abolmaleki P, Soleimani H. Influence of static magnetic field on HeLa and Huo2 cells in the presence of aloe vera extract. Asian Pac J Cancer Prev 2021;22(S1):9–15. https://doi.org/10.31557/APJCP.2021.22.S1.9.

[2] Mata Rocha M, Rodriguez Hernandez RM, Chavez Olmos P, Garrido E, Romero Tlalolini M. Presence of HPV DNA in extracellular vesicles from HeLa cells and cervical samples. Enferm Infecc Microbiol Clin (Engl Ed) 2020;38(4):159 165. https://doi.org/10.1016/j.eimc.2019.06.011.

[3] Bhatia R, Vyas A, El-Bahy SM. Rationale design, synthesis, pharmacological and in-silico investigation of indole-functionalized isoxazoles as antiinflammatory agents. Chemistry Select 2022;(26):1–10. https://doi.org/10.1002/slct.202200800.

[4] Jin S, Bang S, Ahn MA, Lee K, Kim k, Hyun TK, et al. Overproduction of anthocyanin in ginseng hairy roots enhances their antioxidant, antimicrobial, and anti-elastase activities. Kor Soc Plant Biotechnol 2021;(2). https://doi.org/10.5010/JPB.2021.48.2.100.

[5] Peng ZX, Gong XB, Yang Y, Huang LG, Zhang QY, Zhang P, Wan RZ, Zhang BS. Hepatoprotective effect of quercetin against LPS/d GalN induced acute liver injury in mice by inhibiting the IKK/NF kappaB and MAPK signal pathways. Int Immunopharmacol 2017;52:281–9. https://doi.org/10.1016/j.intimp.2017.09.022.

[6] Li S, Wang P, Yang W, Zhao C, Xu H, et al. Characterization of the components and pharmacological effects of mountain-cultivated ginseng and garden ginseng based on the integrative pharmacology strategy. Front Pharmacol 2021;12:659954. https://doi.org/10.3389/fphar.2021.659954.

[7] Samartzi F, Theodosiadou EK, Vainas E, Saratsi A, Tsiligianni T, Rekkas CA, et al. Plasminogen activator activity and plasminogen activator inhibition in the uterus of ewes after the induction of oestrus synchronization or superovulation, involving eCG. Small Rumin Res 2022;210. https://doi.org/10.1016/j.smallrumres.2022.106672.

[8] Sebestyen E, Singh B, Minana B, AmadisA, Francesca P, Mateo. Corrigendum: large scale analysis of genome and transcriptome alterations in multiple tumors unveils novel cancer relevant splicing networks. Genome Res 2018;28(9):1426. https://doi.org/10.1101/gr.242214.118.

[9] Pandey P, Khan F, Farhan M, Jafri A, et al. Elucidation of Rutin role in inducing caspase dependent apoptosis via HPV-E6 and E7 downregulation in cervical cancer HeLa cells. Biosci Rep 2021;41(6). https://doi.org/10.1042/BSR20210670.

[10] Bi YF, Li QY, Tao WM, Tang JX, You GF, Yu L. Ginsenoside Rg1 and ginsenoside Rh1 prevent liver injury induced by acetaminophen in mice. J Food Biochem 2021:e13816. https://doi.org/10.1111/jfbc.13816.

[11] Zarrinnahad H, Mahmoodzadeh A, Hamidi MP, Mahdavi M, Moradi A, Bagheri KP, Shahbazzadeh D. Apoptotic effect of melittin purified from Iranian honey bee venom on human cervical cancer HeLa cell line. Int J Pept Res Ther 2018;24(4):563 570. https://doi.org/10.1007/s1098901796411.

[12] Qin G, Li P, Xue Z. Effect of allyl isothiocyanate on the viability and apoptosis of the human cervical cancer HeLa cell line in vitro. Oncol Lett 2018;15(6):8756–60. https://doi.org/10.3892/ol.2018.8428.

[13] Bian S, Liu M, Yang S, Lu S, Wang S, Bai X, Zhao D, Wang J. 20(S) Ginsenoside Rh2 induced apoptosis and protective autophagy in cervical cancer cells by inhibiting AMPK/mTOR pathway. Biosci Biotechnol Biochem 2021;86(1):92–103. https://doi.org/10.1093/bbb/zbab189.

[14] Song L, Yang F, Wang Z, Zhou Y. Ginsenoside Rg5 inhibits cancer cell migration by inhibiting the nuclear factor kappaB and erythropoietin producing hepatocellular receptor A2 signaling pathways. Oncol Lett 2021;21(6):452. https://doi.org/10.3892/ol.2021.12713.

[15] Xu W, Zhang Q, Ding C, Sun HY, Cao LJ. Gasdermin E derived caspase 3 inhibitors effectively protect mice from acute hepatic failure. Acta Pharmacologica Sinica 2020;42(1). https://doi.org/10.1038/s4140102004342.

[16] Sun Y, Wu J, Dong X, Zhang J, Liu G. MicroRNA 506 3p increases the response to PARP inhibitors and cisplatin by targeting EZH2/beta catenin in serous ovarian cancers. Transl Oncol 2021;14(2):100987. https://doi.org/10.1016/j.tranon.2020.100987.

[17] Li F, Tang X, Xu Y, Wang C, Wang L. A dual protein cascade reaction for the regioselective synthesis of quinoxalines. Org Lett 2020;22(10):3900–4. https://doi.org/10.1021/acs.orglett.0c01186.

[18] Jacomin AC, Petridi S, Di Monaco M, Zambarlal B, Ashish J, Mulakkal NC, Anthimi P, Powell EL, Bonita C, Cleidiane Z. Regulation of expression of autophagy genes by Atg8a interacting partners sequoia, YL 1, and Sir2 in Drosophila. Cell Rep 2020;31(8):107695. https://doi.org/10.1016/j.celrep.2020.107695.

[19] Lee YW, Chen M, Chung IF, Chang TY. lncExplore: a database of pan cancer analysis and systematic functional annotation for lncRNAs from RNA sequencing data. Database (Oxford) 2021. https://doi.org/10.1093/database/baab053.

[20] Zhou B, Lu D, Wang A, Cui J, Zhang L, Li J, Fan L, Wei W, Liu J, Sun G. Endoplasmic reticulum stress promotes sorafenib resistance via miR 188 5p/hnRNPA2B1 mediated upregulation of PKM2 in hepatocellular carcinoma. Mol Ther Nucleic Acids 2021;26:1051–65. https://doi.org/10.1016/j.omtn.2021.09.014.

[21] Yu Y, Wu D, Li Y, Hui Q, Zheng S. Ketamine enhances autophagy and endoplasmic reticulum stress in rats and SV HUC 1 cells via activating IRE1 TRAF2 ASK1 JNK pathway. Cell Cycle 2021;20(18):1907–22. https://doi.org/10.1080/15384101.2021.1966199.

[22] Liu K, Chen Y, Ai F, Li YQ, Zhang WT. PHLDA3 inhibition attenuates endoplasmic reticulum stress induced apoptosis in myocardial hypoxia/reoxygenation injury by activating the PI3K/AKT signaling pathway. Exp Ther Med 2021;21(6):613. https://doi.org/10.3892/etm.2021.10045.

[23] Dong JY, Xia KJ, Liang W, Liu LL, Chen DP. Ginsenoside Rb1 alleviates colitis in mice via activation of endoplasmic reticulum resident E3 ubiquitin ligase Hrd1 signaling pathway. Acta Pharmacol Sin 2021;42(9):1461 1471. https://doi.org/10.1038/s41401020005619.

[24] Yorifuji H, Arase N, Kohyama M, Hirano T, Suenaga T, Kumanogoh A, Arase H. Transport of cellular misfolded proteins to the cell surface by HLA B27 free heavy chain. Biochemical and Biophysical Research Communications 2019;511(4). https://doi.org/10.1016/j.bbrc.2019.02.120.

[25] Liu C, Huang S, Wang X, Huang S. The otubain YOD1 suppresses aggregation and activation of the signaling adaptor MAVS through Lys63 linked deubiquitination. J Immunol 2019;202(10):2957–70. https://doi.org/10.4049/jimmunol.1800656.

[26] Wang S, Mo Y, Midorikawa K, Zhang Z, Murata M. The potent tumor suppressor miR 497 inhibits cancer phenotypes in nasopharyngeal carcinoma by targeting ANLN and HSPA4L. Oncotarget 2015;6(34):35893–907. https://doi.org/10.18632/oncotarget.5651.

[27] Tang Y, Tang R, Tang M, Huang P, Nie S. LncRNA DNAJC3 AS1 regulates fatty acid synthase via the EGFR pathway to promote the progression of colorectal cancer. Front Oncol 2020;10:604534. https://doi.org/10.3389/fonc.2020.604534.

[28] Wan X, Zhu L, Zhao L, Peng L, Chen K. hPER3 promotes adipogenesis via hHSP90AA1 mediated inhibition of Notch1 pathway. Cell Death Dis 2021;12(4):301. https://doi.org/10.1038/s41419021035840.